

We examine the difference of morphology in tilted columnar W films.

Columns are composed of a dense microstructure in front of the W particle flux.

A fibrous and bundled feature appears in the shadowing zone of the columns.

These morphological disparities are connected to the energy transfer of W atoms to the column apex.

## A 4-view imaging to reveal microstructural differences in obliquely sputter-deposited tungsten films

1 Raya EL BEAINOU<sup>1</sup>, Aurelio GARCIA-VALENZUELA<sup>2</sup>, Marina RASCHETTI<sup>1</sup>, Jean-Marc COTE<sup>1</sup>, Rafael  
2  
3 ALVAREZ<sup>2,3</sup>, Alberto PALMERO<sup>2</sup>, Valérie POTIN<sup>4</sup>, Nicolas MARTIN<sup>1,a)</sup>  
4

5  
6 <sup>1</sup> Institut FEMTO-ST, UMR 6174, Univ. Bourgogne Franche-Comté, 15B, Avenue des montboucons, 25030  
7  
8 BESANCON Cedex, France  
9

10 <sup>2</sup> Instituto de Ciencia de Materiales de Sevilla (CSIC-Universidad de Sevilla), Americo Vespucio 49, 41092 SEVILLA,  
11  
12 Spain  
13

14 <sup>3</sup> Departamento de Física Aplicada I. Escuela Politécnica Superior, Universidad de Sevilla, c/ Virgen de África 7, 41011  
15  
16 Seville, Spain  
17

18 <sup>4</sup> Laboratoire Interdisciplinaire Carnot de Bourgogne (ICB), UMR 6303, Univ. Bourgogne Franche-Comté, 9, Avenue  
19  
20 Alain Savary, BP 47870, 21078 DIJON Cedex, France  
21  
22  
23

### 24 **Abstract**

25  
26 We report on the morphological disparity of the columnar growth in W thin films sputter-deposited by oblique angle  
27  
28 deposition. Oriented tungsten thin films (400 nm thick) are prepared using a tilt angle  $\alpha$  of 80° and a sputtering pressure  
29  
30 of 0.25 Pa. Inclined columns ( $\beta = 40^\circ$ ) are produced and the microstructure is observed by scanning electron  
31  
32 microscopy. A 4-view imaging is performed in order to show inhomogeneous growing evolutions in the columns.  
33  
34 Morphological features vs. viewing direction are also investigated from a growth simulation of these tilted W columns.  
35  
36 Experimental and theoretical approaches are successfully compared and allow understanding how the direction of the W  
37  
38 particle flux leads to dense or fibrous morphologies, as the column apexes are in front of the flux or in the shadowing  
39  
40 zone.  
41

42 **Keywords:** Oblique angle deposition, W thin films, tilted columns, dense, fibrous morphology.  
43  
44  
45

### 46 **1. Introduction**

47  
48 For this last ten years, oblique angle deposition (OAD) has turned out into an attractive strategy to produce  
49  
50 nanostructured thin films with tunable morphologies [1-3]. The growth of original architectures obtained by vacuum  
51  
52 processes (evaporation and/or sputtering) at oblique angles has become a hot topic for the development of a large variety  
53  
54 of applications [4-7]. Many investigations were conducted by electron microscopy that enabled a direct analysis of the  
55  
56 film morphology at high resolution. It was clearly shown that the atomic-scale shadowing phenomenon appeared as a  
57  
58 crucial factor in the film growth and the development of columnar morphologies with asymmetric microstructures (e.g.  
59  
60

---

61  
62 <sup>a)</sup> Corresponding author: nicolas.martin@femto-st.fr; Tel.: +33 (0)3 63 08 24 31; Fax: +33 (0)3 81 85 39 98  
63  
64  
65

column fanning) leading to significant anisotropic physical properties. As a result, all reports in the literature have mainly been focused on cross-section and/or top views of tilted columnar architectures [8-10]. To the best of our knowledge, very few studies have been devoted to view from all facets, especially oppositely or in the direction of the particle flux [11].

In this letter, we show that the morphology of each tilted column in obliquely sputter-deposited W films is strongly influenced by the direction of the particle flux. Experimental and simulated results both demonstrate that dense and fibrous morphologies are simultaneously and oppositely produced in a given column. These dissimilar features are directly related to some differences of growth mechanisms connected to an energetic transfer of W atoms when they impinge on the column apex.

## 2. Material and methods

The tungsten thin films were deposited by DC magnetron sputtering in a 40 L homemade chamber at a base pressure below  $10^{-5}$  Pa [12]. A tungsten metallic target with a purity of 99.9 at % and a diameter of 51 mm, was used. The current of the tungsten target was fixed at  $I_w = 140$  mA. All films were sputtered with an argon flow rate of 2.4 sccm and a pumping speed of  $26 \text{ L s}^{-1}$  leading to an argon sputtering pressure  $p = 0.25$  Pa. (100) silicon substrates were fixed at the center of the substrate holder. The latter was inclined at an angle  $\alpha$  of  $80^\circ$ . The substrate-to-target centers distance was  $d_{w,s} = 65$  mm. The time of deposition was adjusted in order to get a film thickness close to 400 nm. The morphology (top and fractured cross-section views) of W films was observed by scanning electron microscopy (SEM) in a Dual Beam SEM/FIB FEI Helios 600i microscope.

A well tested model [13] was used to simulate the growth of tilted W films. Such a home-made Monte Carlo code is of special interest to understand the fundamental mechanisms and the resulting morphology of W films sputter-deposited at an oblique angle. This software performs simulations of the film formation taking into account geometrical constraints and operating conditions and considers different atomistic processes such as surface shadowing and kinetic energy-induced mobilization processes during the deposition process. It has already been presented in detail and several former studies support its validity to precisely describe the growth and columnar features of various materials [13-16].

## 3. Results and discussion

Figure 1 is a 4-view imaging obtained by SEM (with secondary electrons) of W thin films sputter-deposited with an angle  $\alpha$  of  $80^\circ$ . Top view (a), cross-section view (b), front (c) and opposite (d) sides of the W particle flux clearly show different morphologies of the columnar structure. As previously reported for most of obliquely deposited films [17], elongated column cross-sections (elliptical shape) along the direction perpendicular to the incident flux ( $y$ -direction) are clearly seen from the top view (Fig. 1 a). This morphological asymmetry, namely column fanning, is connected to

anisotropic physical properties of obliquely deposited films and come from the one-dimensional nature of the shadowing effect. For the first growing stage, the cross-section is roughly symmetric in the  $x$ - (parallel to the flux) and  $y$ - (perpendicular to the flux) directions. As the film's thickness increases, shadowing effect prevents broadening along  $x$  and the column features gradually fan out along the  $y$ -axis. The tilted columns apex interestingly shows a rather crescent than elliptical shape. Fanning of the individual columns and their lateral growth allow neighboring columns to be connected to each other and chain together, whereas shadowing prevents column merging along the  $x$ -direction. This produces a preferential bundling of the columnar microstructure in the  $y$ -direction. As a result, fanning and chaining phenomena lead to elongated and fan-like columnar morphology. It is also worth noting that the column apex in front of the particle flux seems to be smoother and denser (abrupt edge) than the opposite side, which exhibits a serrated edge and a fibrous feature.

The typical column tilt angle  $\beta$ , defined as the angle between the substrate normal and the column center axis, reaches  $40^\circ$  for our sputtering conditions (Fig. 1 b), which is (as expected) less than the deposition angle  $\alpha = 80^\circ$ . Of relevance is the shape of the column apex where the side facing the particle flux again appears dense with a domed cross-section. This cross-section view supports the anisotropic morphology earlier imaged from the top view. SEM observations performed facing the flux (Fig. 1c) and in the shadowing zone (Fig. 1d) corroborate the difference of columnar shape, i.e. a smooth and a ragged edge, respectively. No clear structure can be seen from the facing view and this columns side appears as dense and smooth. The opposite side (in the shadowing zone) distinctly exhibits a more fibrous and bundled columnar morphology as shown in Fig. 1d. Fanned columns are obtained, which are composed of bundled and narrow columns. This column side is rough and elongated in the direction of the particle flux.

In order to understand these differences of morphology, simulations of the columnar growth have been carried out using the same approach as the SEM observations, i.e. a 4-view imaging of the tilted columnar structure (Fig. 2). The top view of the simulated surface similarly shows an elongated shape of the column cross-section, normal to the particle flux (Fig. 2a). The column fanning phenomenon leads to the chaining of adjacent columns, which well correlates with experimental observations in Fig. 1a. The crescent-like shape of the column apex and the preferential bundling of the columnar microstructure in the  $y$ -direction can be noticed. It is also worth noting that the column side facing the particle flux is more abrupt than the opposite side. This difference of morphology is even more viewable from the simulated cross-section observation (Fig. 2b). The tilted columns clearly show a smooth contour in front of the particle flux, whereas a rough and irregular profile is produced on the opposite side. Fig. 2c and 2d corroborate these unlike profiles and well agree with SEM experiments (Fig. 1c and 1d). A dense and smooth column side facing the flux, against a rough and fibrous structure on the other side. As a result, simulations give rise to realistic representations of  $W$  tilted columnar films and is a valuable tool for predicting the film morphology of the top, cross-section and two sides of the oriented columnar architecture.

1  
2  
3  
4  
5  
6  
7  
8  
9  
10  
11  
12  
13  
14  
15  
16  
17  
18  
19  
20  
21  
22  
23  
24  
25  
26  
27  
28  
29  
30  
31  
32  
33  
34  
35  
36  
37  
38  
39  
40  
41  
42  
43  
44  
45  
46  
47  
48  
49  
50  
51  
52  
53  
54  
55  
56  
57  
58  
59  
60  
61  
62  
63  
64  
65

In figure 3, we analyze the origin of the smooth and fibrous structures on both sides of the nanocolumns. To this aim, we have used the solution of the model shown in figure 2 to throw virtual deposition atoms towards this static surface and calculated the average energy flux arriving at each position. This is shown in figure 3a where we can see that this energy flux is not distributed homogeneously over the surface. In fact, and due to the ballistic nature of the deposition, it is higher at the front part of the nanocolumns, suggesting a direct correlation between the kinetic energy flux and the appearance of smooth/fibrous structures. In figures 3b and 3c, respectively, we show the top and cross-sectional views of the kinetic energy-induced mobility vector on the framed column in figure 3a. It is interesting to notice that the kinetic energy of the W atoms is directly transferred to the column apex straightly oriented in front of the flux, where heavy W atoms act as a hammer leading to a curved profile of the apex (Fig. 3c). As a result, a dense material is produced in the front part of the column. Moreover, W atoms hitting the column apex close to the shadowing zone are able to induce mobility in the direction of the particle flux (Fig. 3c), which tend to separate material from this dense region causing the formation of nucleation centers that generate the fibrous structures upon growth. The resulting morphology is therefore composed of bundled nano-columns more or less connected to each other. A serrated edge combined with a porous structure are rather formed on this column side as revealed in Fig. 3c.

#### 4. Conclusions

W thin films have been prepared by DC magnetron sputtering using a deposition angle of  $80^\circ$  and an argon pressure of 0.25 Pa. A typical tilted columnar microstructure has been produced with an elongated shape of the columns cross-section (fanning effect) along the direction perpendicular to the incident particle flux. A 4-view imaging by SEM has been performed in order to show some significant differences of the columns feature depending on their orientation to the incoming W atoms. It has been demonstrated that a smooth and dense morphology is produced on the columns side in front of the flux, whereas a porous, rough and fibrous aspect is rather obtained on the opposite side. A simulation analysis via a Monte Carlo approach has similarly been performed focusing observations of the column morphology following the same four directions, i.e. top, cross-section, facing and opposite to the flux. The compact part on the column side facing the flux is connected to the energy transfer of W atoms (ballistic behavior). They impinge on the column apex and are abruptly stopped leading to a dense material. On the opposite side located in the shadowing zone, a few parts of W atoms arrive with a grazing incidence. They hit the column apex close to the shadowing zone and induce atomic mobility processes in the direction of the flux. Bundled nano-columns exhibiting a porous structure and a rough surface are formed.

#### Acknowledgements

This work was supported by the EIPHI Graduate School (contract ANR-17-EURE-0002), the Region of Bourgogne Franche-Comté and the French RENATECH network.

## References

- [1] K. Robbie, M.J. Brett, Sculptured thin films and glancing angle deposition: Growth mechanics and applications, *J. Vac. Sci. Technol. Vac.*, 15 (1997) 1460–1465. doi:10.1116/1.580562.
- [2] A. Barranco, A. Borrás, A.R. González-Elipé, A. Palmero, Perspectives on oblique angle deposition of thin films: From fundamentals to devices, *Prog. Mater. Sci.*, 76 (2016) 59-153. <https://doi.org/10.1016/j.pmatsci.2015.06.003>.
- [3] M.M. Hawkeye, M.T. Taschuk, M.J. Brett, *Glancing Angle Deposition of thin films: Engineering the nanoscale*, John Wiley & Sons, Ltd, Chichester, UK, 2014. <https://doi.org/10.1002/9781118847510>.
- [4] Y.P. Zhao, D.X. Ye, G.C. Wang, T.M. Lu, Designing nanostructures by glancing angle deposition, *Proc. SPIE*, 5219 (2003) 59-73. <https://doi.org/10.1117/12.505253>.
- [5] B. Mohanty, B.D. Morton, A. Sinan Alagoz, T. Karabacak, M. Zou, Frictional anisotropy of tilted molybdenum nanorods fabricated by glancing angle deposition, *Tribol. Int.* 80 (2014) 216–221. <https://doi.org/10.1016/j.triboint.2014.07.010>.
- [6] M.S. Rodrigues, J. Borges, M. Proença, P. Pedrosa, N. Martin, K. Romanyuk, A.L. Kholkin, F. Vaz, Nanoplasmonic response of porous Au-TiO<sub>2</sub> thin films prepared by oblique angle deposition, *Nanotechnology*, 30 (2019) 225701. <https://doi.org/10.1088/1361-6528/ab068e>.
- [7] X. Xu, M. Pour Arab Yazdi, J.B. Sanchez, A. Billard, F. Berger, N. Martin, Exploiting the dodecane and ozone sensing capabilities of nanostructured tungsten oxide films, *Sensor Actuat. B-Chem.*, 266 (2018) 773-783. <https://doi.org/10.1016/j.snb.2018.03.190>
- [8] C. Grüner, S. Liedtke, J. Bauer, S.G. Mayr, N. Rauschenbach, Morphology of thin films formed by oblique physical vapor deposition, *ACS Nano Mater.*, 1 (2018) 1370-1376. <https://doi.org/10.1021/acsanm.8b00124>.
- [9] E. Coffy, G. Dodane, S. Euphrasie, A. Mosset, P. Vairac, N. Martin, H. Baida, J.M. Rampnoux, S. Dilhaire, Anisotropic propagation imaging of elastic waves in oriented columnar thin films, *J. Phys. D: Appl. Phys.*, 50 (2017) 484005. <https://doi.org/10.1088/1361-6463/aa92ad>.
- [10] J. Dervaux, P.A. Cormier, P. Moskovkin, O. Douheret, S. Konstantinidis, R. Lazzaroni, S. Lucq, R. Snyders, Synthesis of nanostructured Ti thin films by combining glancing angle deposition and magnetron sputtering: A joint experimental and modeling study, *Thin Solid Films*, 636 (2017) 644-657. <https://doi.org/10.1016/j.tsf.2017.06.006>.
- [11] T. Brown, K. Robbie, Observations of self-assembled microscale triangular-shaped spikes in copper and silver thin films, *Thin Solid Films*, 531 (2013) 103-112. <https://doi.org/10.1016/j.tsf.2012.12.118>
- [12] P. Pedrosa, A. Ferreira, J.M. Cote, N. Martin, M. Arab Pour Yazdi, A. Billard, S. Lanceros-Mendez, F. Vaz, Influence of the sputtering pressure on the morphological features and electrical resistivity anisotropy of nanostructured titanium films, *Appl. Surf. Sci.*, 420 (2017) 681-690. <https://doi.org/10.1016/j.apsusc.2017.05.175>.

- [13] R. Alvarez, J.M. Garcia-Martin, A. Garcia-Valenzuela, M. Macias-Montero, F.J. Ferrer, J. Santiso, V. Rico, J. Cotrino, A.R. Gonzalez-Elipe, A. Palmero, Nanostructured Ti thin films by magnetron sputtering at oblique angles, *J. Phys. D: Appl. Phys.*, 49 (2016) 045303. <https://doi.org/10.1088/0022-3727/49/4/045303>.
- [14] R. Alvarez, J.M. Garcia-Martin, M. Macias-Montero, L. Gonzalez-Garcia, J.C. Gonzalez, V. Rico, J. Perlich, J. Cotrino, A.R. Gonzalez-Elipe, A. Palmero, Growth regimes of porous gold thin films deposited by magnetron sputtering at oblique incidence: From compact to columnar microstructures, *Nanotechnology*, 24 (2013) 045604. <https://doi.org/10.1088/0957-4484/24/4/045604>.
- [15] A. Garcia-Valenzuela, C. Lopez-Santos, R. Alvarez, V. Rico, J. Cotrino, A.R. Gonzalez-Elipe, A. Palmero, Structural control in porous/compact multilayer systems grown by magnetron sputtering, *Nanotechnology* 28 (2017) 465605. <https://doi.org/10.1088/1361-6528/aa8cf4>.
- [16] A. Garcia-Valenzuela, S. Muñoz-Piña, G. Alcala, R. Alvarez, B. Lacroix, A.J. Santos, J. Cuevas-Maraver, V. Rico, R. Gago, L. Vazquez, J. Cotrino, A.R. Gonzalez-Elipe, A. Palmero, Growth of nanocolumnar thin films on patterned substrates at oblique angles, *Plasma Process. Polym.*, 16 (2019) 1-10. <https://doi.org/10.1002/ppap.201800135>.
- [17] N. Martin, J. Sauget, T. Nyberg, Anisotropic electrical resistivity during annealing of oriented columnar titanium films, *Mater. Lett.* 105 (2013) 20–23. <https://doi:10.1016/j.matlet.2013.04.058>.

### Figure captions

#### Figure 1

SEM observations of a) top, b) cross-section, c) facing and d) opposite views to the particle flux of a 400 nm thick W film sputter-deposited with an inclination angle  $\alpha = 80^\circ$ . White arrows and symbols indicate the direction of the particle flux.

#### Figure 2

The same views as in Fig. 1 of simulated W films, i.e. a) top, b) cross-section, c) facing and d) opposite to the particle flux.

#### Figure 3

Calculated images of the simulated W films. a) Average flux of kinetic energy of deposition species on the film surface. Average kinetic energy displacement vector of surface atoms in the framed nanocolumn, b) top and c) cross-section views.



Figure 1

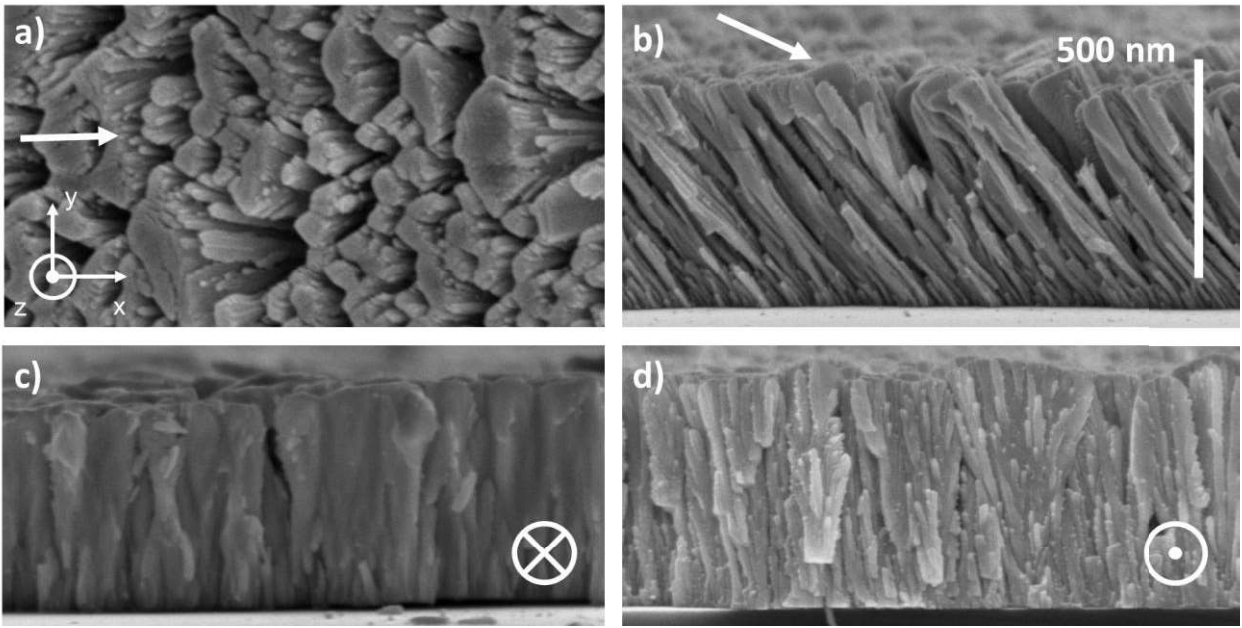


Figure 2

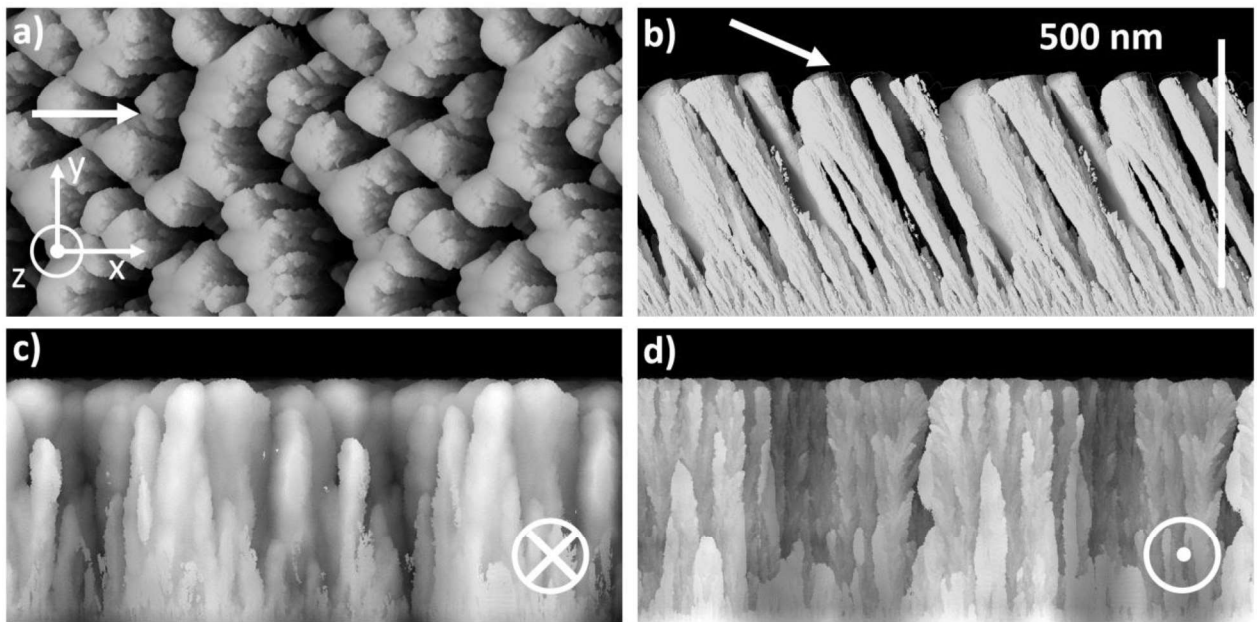


Figure 3

1  
2  
3  
4  
5  
6  
7  
8  
9  
10  
11  
12  
13  
14  
15  
16  
17  
18  
19  
20  
21  
22  
23  
24  
25  
26  
27  
28  
29  
30  
31  
32  
33  
34  
35  
36  
37  
38  
39  
40  
41  
42  
43  
44  
45  
46  
47  
48  
49  
50  
51  
52  
53  
54  
55  
56  
57  
58  
59  
60  
61  
62  
63  
64  
65

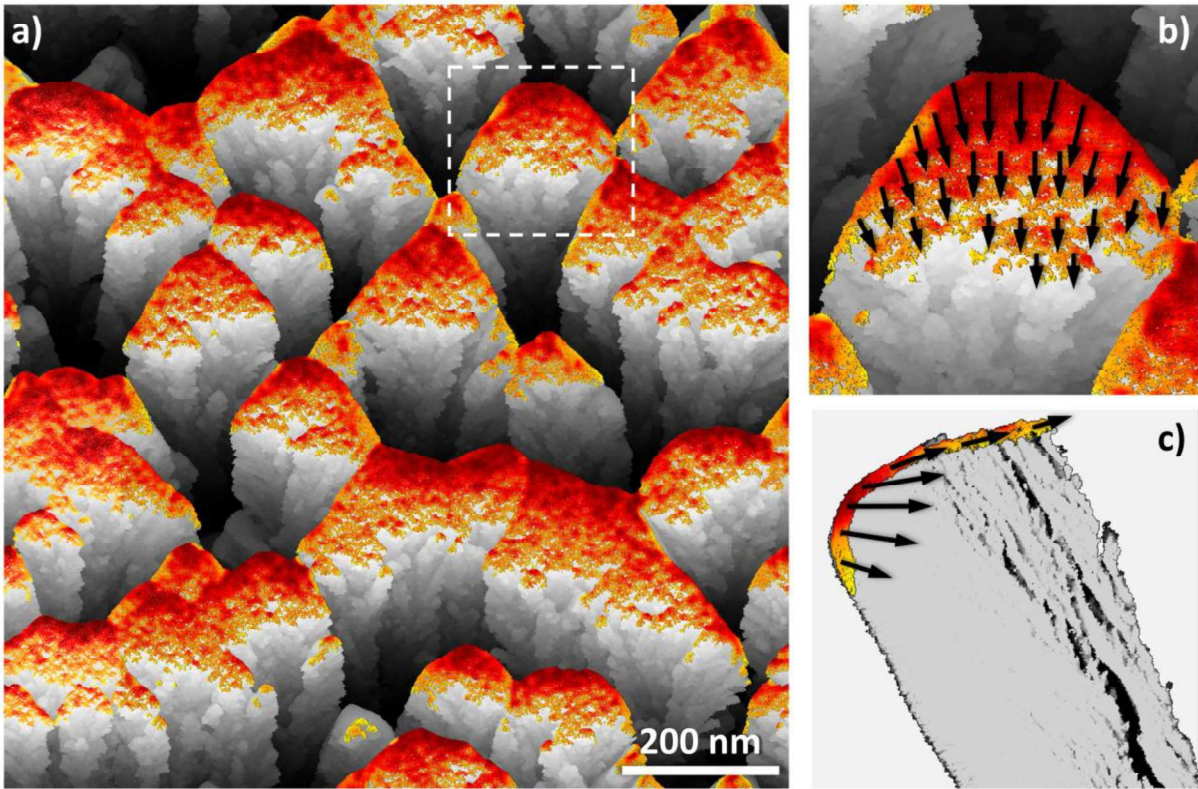


Figure1  
[Click here to download high resolution image](#)

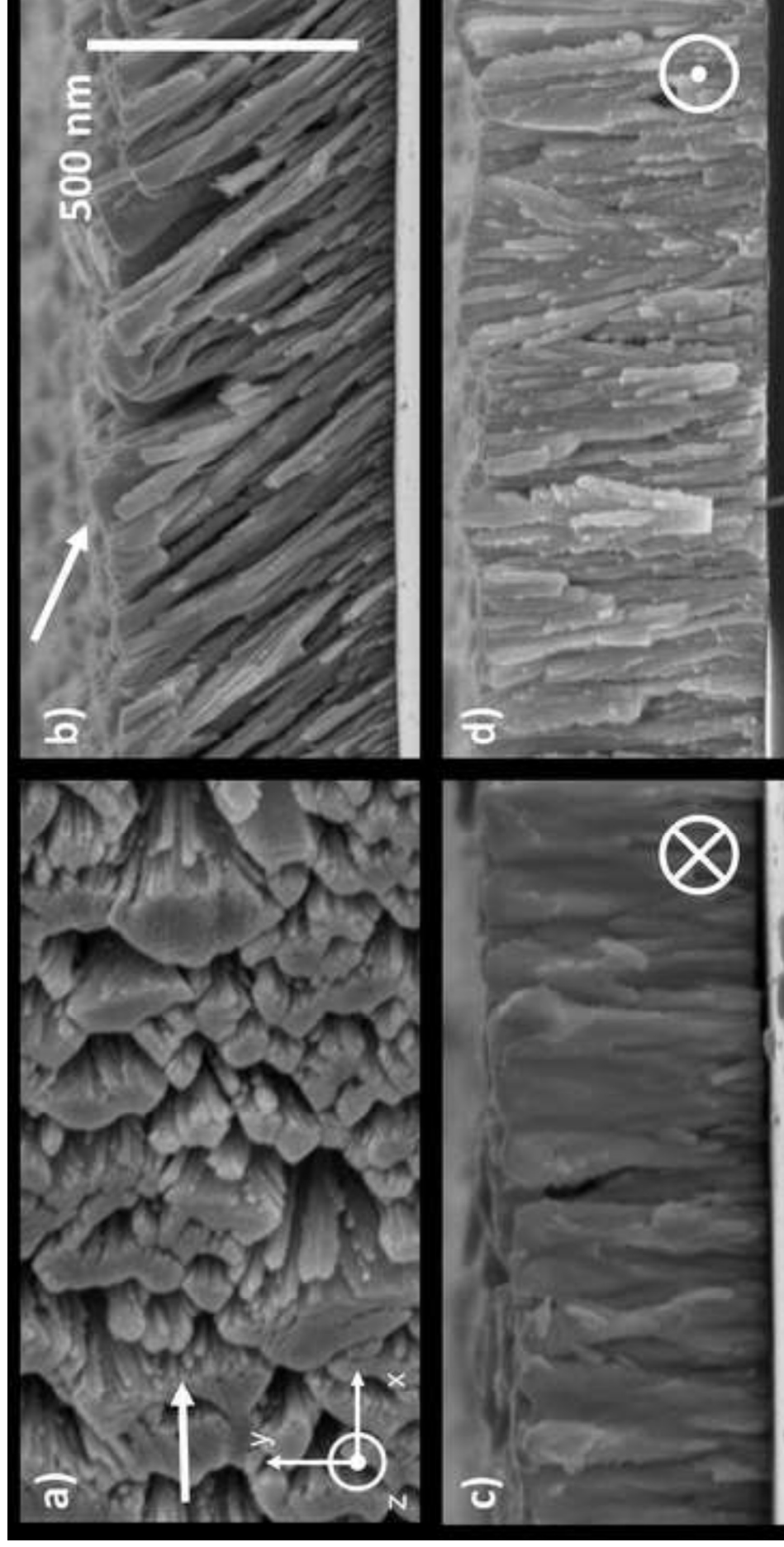




Figure2  
[Click here to download high resolution image](#)

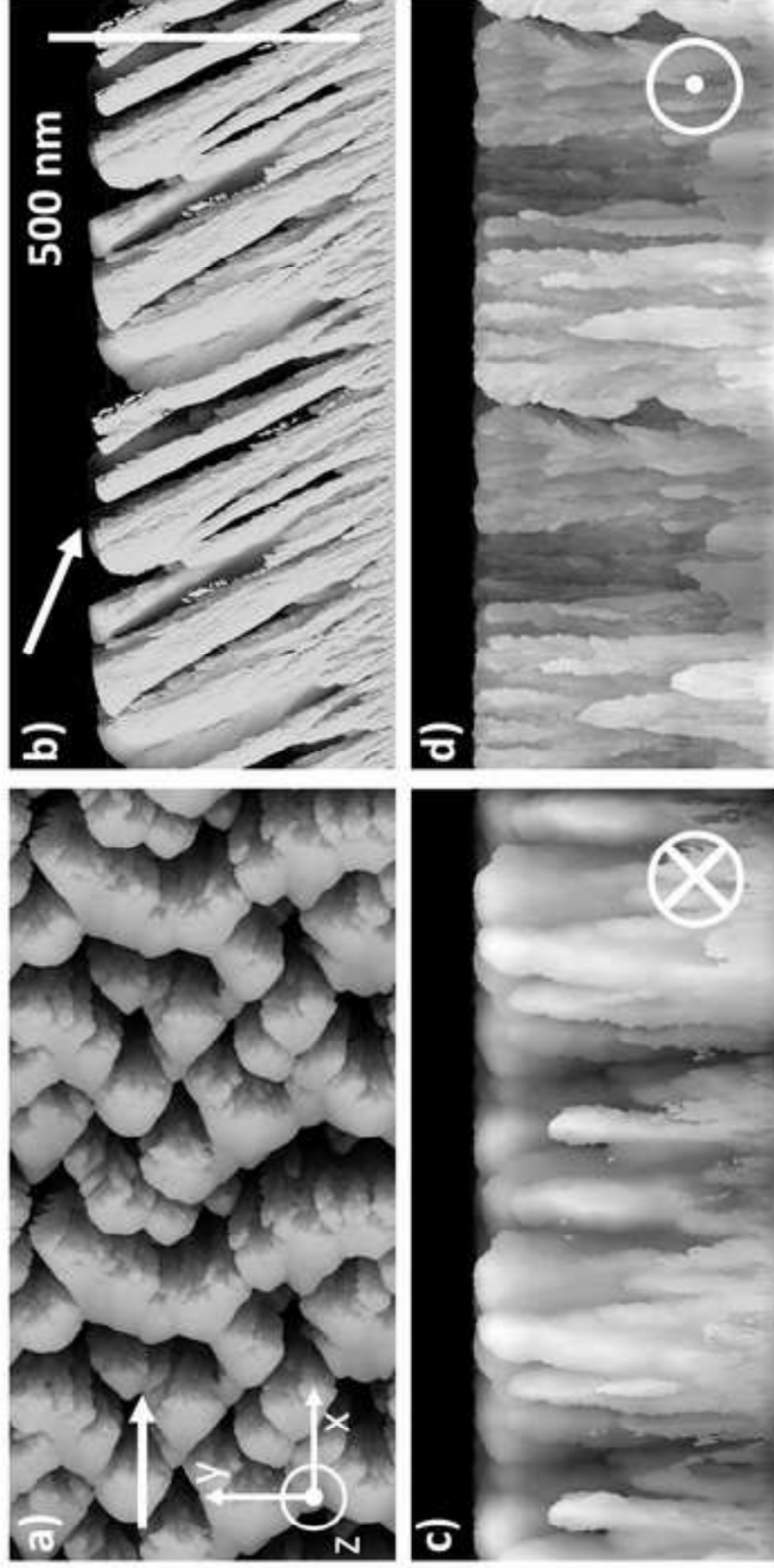
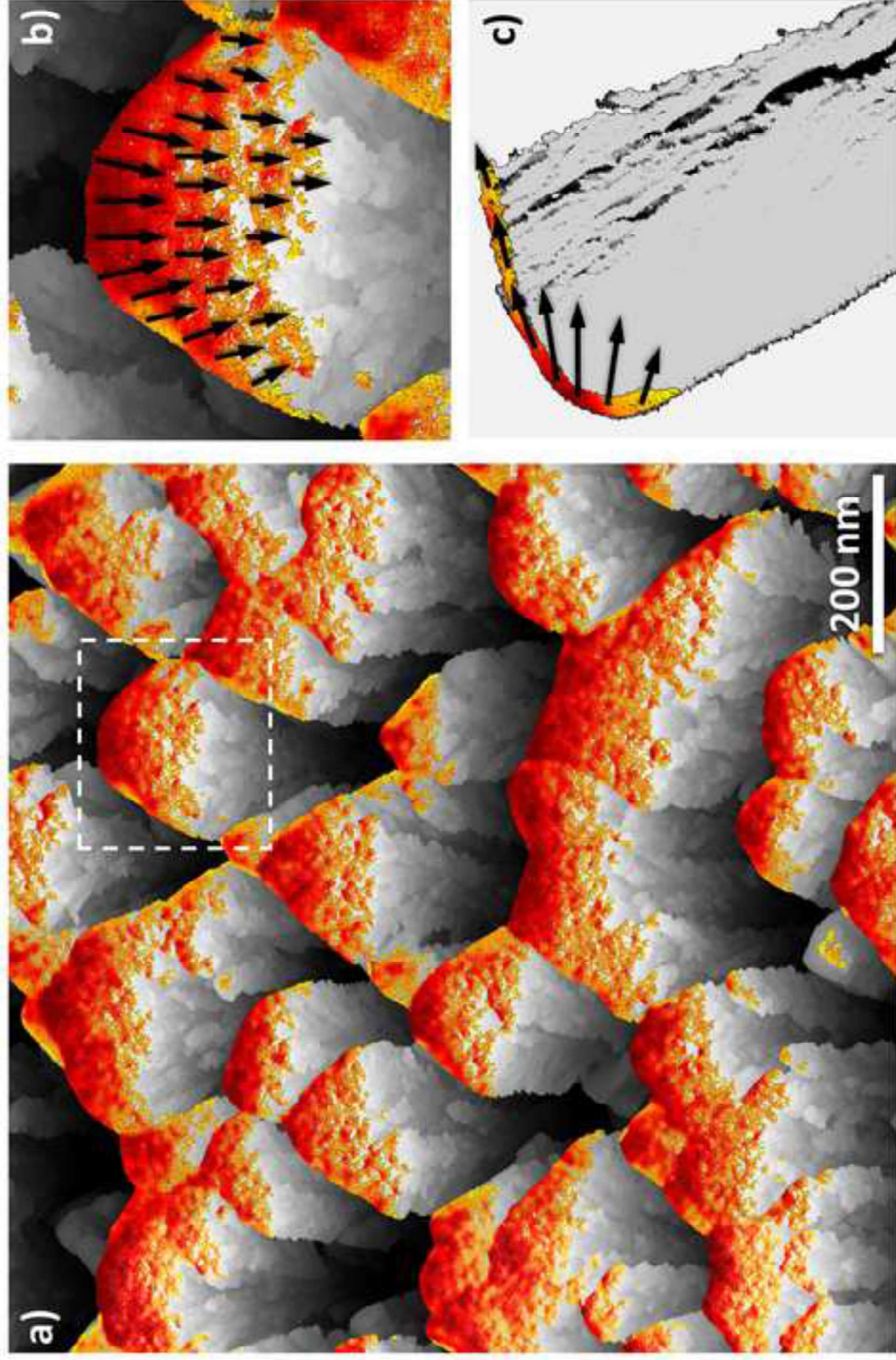



Figure3  
[Click here to download high resolution image](#)



**Declaration of interests**

The authors declare that they have no known competing financial interests or personal relationships that could have appeared to influence the work reported in this paper.

The authors declare the following financial interests/personal relationships which may be considered as potential competing interests:



**\*Conflict of Interest**

[Click here to download Conflict of Interest: Conflict\\_of\\_Interest.pdf](#)